ISSN (Print) 1225-9918
ISSN (Online) 2287-3406
Journal of Life Science **2020** Vol. 30. No. 4. 331~342 DOI : https://doi.org/10.5352/JLS.2020.30.4.331

Inhibitory Effects of *Asparagus cochinchinensis* in LPS-Stimulated BV-2 Microglial Cells through Regulation of Neuroinflammatory Mediators, the MAP Kinase Pathway, and the Cell Cycle

Hyun Ah Lee[1], Ji Eun Kim[1], Jun Young Choi[1], Ji Eun Sung[1], Woo Bin Youn[1], Hong Joo Son[2,4], Hee Seob Lee[3,4], Hyun-Gu Kang[5] and Dae Youn Hwang[1,4*]

[1]*Department of Biomaterials Science, College of Natural Resources and Life Science/Life and Industry Convergence Research Institute, Pusan National University, Miryang 50463, Korea*
[2]*Department of Life Science & Environmental Biochemistry, College of Natural Resources and Life Science/Life and Industry Convergence Research Institute, Pusan National University, Miryang 50463, Korea*
[3]*Department of Food Science and Nutrition, College of Human Ecology, Pusan National University, Busan 46241, Korea*
[4]*Wellbeing Product Regional Innovation System Center, Pusan National University, Miryang 50463, Korea*
[5]*Veterinary Medical Center, Department of Veterinary Theriogenology, College of Veterinary Medicine, Chungbuk National University, Cheongju 28644, Korea*

Received December 10, 2019 / Revised February 26, 2020 / Accepted February 28, 2020

The suppression of neuroinflammatory responses in microglial cells can be considered a key target for improving the progression of neurodegenerative diseases such as Alzheimer's disease (AD), Parkinson's disease (PD), and Huntington's disease (HD). *Asparagus cochinchinensis* has traditionally been used as a medicine to treat fever, cough, kidney disease, breast cancer, inflammatory diseases, and brain diseases. In this study, we investigated the neuroprotective mechanism of an aqueous extract from *A. cochinchinensis* root (AEAC), particularly its anti-inflammatory effects on lipopolysaccharide (LPS)-activated BV-2 microglial cells. BV-2 cells were treated with four different concentrations of AEAC. No significant toxicity was detected in BV-2 cells treated with AEAC. Nitric oxide (NO), cyclooxygenase-2 (COX-2) mRNA, and inducible nitric oxide synthase (iNOS) mRNA levels were 21% lower in the AEAC+LPS group than in the Vehicle+LPS group. Lower proinflammatory (TNF-α and IL-1β) and anti-inflammatory cytokine (IL-6 and IL-10) levels were also detected in the AEAC+LPS group than in the Vehicle+LPS group, albeit at varying rates. Moreover, the phosphorylation of mitogen-activated protein kinase (MAPK) members after LPS treatment was significantly recovered in the AEAC-pretreated group compared to the Vehicle+LPS group, enhancement of the phosphorylation of mitogen-activated protein kinase (MAPK) members after LPS treatment was significantly recovered in the AEAC-pretreated group, while cell cycle arrest at the G2/M phase caused by LPS treatment was less severe in the AEAC+LPS group. The increase in reactive oxygen species (ROS) generation induced by LPS treatment was also lower in the AEAC-pretreated group than in the Vehicle+LPS group. This is the first study to show that AEAC exerts anti-neuroinflammatory activity against LPS stimulation by regulating the MAPK signaling pathway, the cell cycle, and ROS production.

Key words : Anti-neuroinflammation, *Asparagus cochinchinesis*, COX-2, cytokines, NO

Introduction

Neuroinflammatory response is a critical defense mechanism to pathogens, toxic metabolites, autoimmunity or neuronal tissue damage in central nervous system (CNS). This reaction is widely regarded as chronic inflammation characterized by the activation of microglia and recruitment of other immune cells into the brain [4]. During these responses, activated microglia cells undergo significant morphological change from resting ramified cells to motile amoeboid cells while releasing pro-inflammatory cytokines and cytotoxic factors such as nitric oxide (NO), tumor necrosis factor-*a* (TNF-α), Interleukin (IL)-1b and cyclooxygenase-2 (COX-2) [26, 27]. The activation of these cells is also closely related to the pathogenesis of various neurodegenerative diseases, including Alzheimer's disease (AD), Huntington's disease (HD) and Parkinson's disease (PD) [2, 7]. Therefore, the con-

***Corresponding author**
Tel : +82-55-350-5388, Fax : +82-55-350-5389
E-mail : dyhwang@pusan.ac.kr

trol of over-activated microglia cells is considered a potential therapeutic target to alleviate the progression of these neurological diseases.

The root of *A. cochinchinesis* has long been considered a therapeutic drug owing to its anti-inflammatory, diuretic, antiseptic, antitussive, antibacterial, nervine, sialogoue, antipyretic, and stomachic effects. These roots are administered in combination with other herbs as medicine to treat lung disease, immune system related diseases and aging [40, 41]. Recently, there has been increasing scientific evidence that extract of *A. cochinchinesis* leads to an anti-inflammatory response via the regulation of key mediators. Treatment with *A. cochinchinesis* extract significantly inhibited the secretion of the pro-inflammatory cytokines such as TNF-α in LPS- and substance P-stimulated mouse astrocytes [13]. Moreover, the NO concentration effectively decreased in response to Compounds 2, 3 and 4 among seven compounds isolated from *A. cochinchinesis* extract in lipopolysaccharide (LPS)-stimulated BV-2 microglial cells. Moreover, ethanol extract from *A. cochinchinesis* greatly decreased the degree of ectopic edema, ear thickness, cytokine secretion, and myeloperoxidase activity, which are considered indicators of skin inflammation progression, in a skin inflammation-induced mouse model treated with 12-O-tetradecanoyl-phorbol-13-acetate [35]. The crude aqueous extract of *A. cochinchinensis* also effectively inhibits TNF-α–induced cytotoxicity [28], while increasing the spleen index and superoxide dismutase (SOD) activity and decreasing malondialdehyde in mice [41]. Moreover, a recent study reported the inhibitory effects of *A. cochinchinensis* in allergic asthma-associated airway remodeling. The standardized herbal formula PM014, which includes the roots of *A. cochinchinensis*, efficiently inhibited the number of total cells, eosinophils, neutrophils, macrophages and lymphocytes in the bronchoalveolar lavage fluid of cockroach allergen-induced mice [11]. However, the protective effects of *A. cochinchinensis* against LPS-stimulated neuroinflammation of microglia through the inhibition of inflammatory mediators, as well as the MAPK signaling pathway, cell cycle and reactive oxygen species (ROS) production have not been fully investigated.

Therefore, in this study, we investigated the fundamental mechanisms responsible for anti-neuroinflammatory activities of aqueous extract from *A. cochinchinesis* root (AEAC) in LPS-induced BV-2 microglia cells to provide scientific evidence of the potential for use of AEAC in therapeutic drugs against neurodegenerative disorders.

Materials and Methods

Preparation of AEAC

The AEAC used in this study was prepared as previously described [16]. Briefly, the roots of *A. cochinchinensis* were collected from plantations in the Go-Chang area in Korea and identified by Dr. Shin Woo Cha at the Herbal Crop Research Division, National Institute of Horticultural & Herbal Science. After drying using a drying machine (FD 5510S-FD5520S, Ilshinbiobase Co., Dongducheon, Korea), the AEAC were deposited as voucher specimens of GR (WPC-14-003) in the functional materials bank of the PNU-Wellbeing RIS Center at Pusan National University. Dry roots were reduced to powder using a pulverizer (MF-3100S, Hanil Electric Co., Seoul, Korea), after which AEAC was obtained at 121℃ for 45 min in a fixed liquor ratio (solid powder of *A. cochinchinensis*/dH_2O ratio, 75 g: 500 ml) using circulating extraction equipment (Woori Science Instrument Co., Pocheon, Korea) (Fig. 1A). The extract solutions were subsequently passed through a filter membrane (Whatman No.

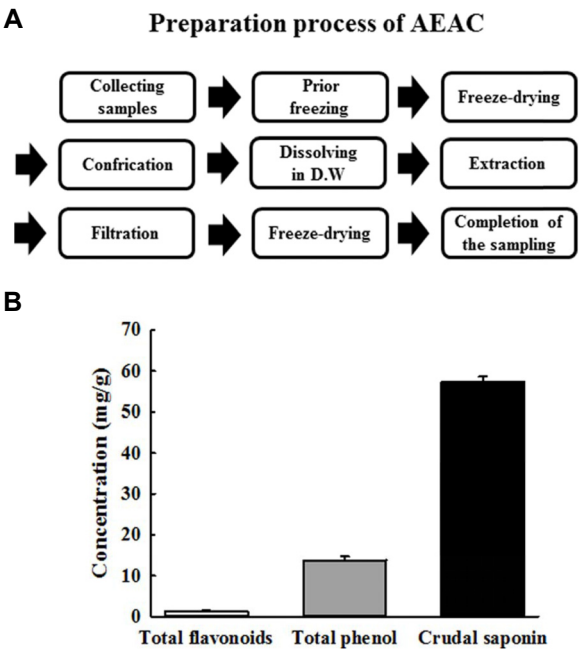

Fig. 1. Preparation of AEAC and level of its bioactive compounds. (A) AEAC was obtained from the root of *A. cochinchinensis* using distilled water under the conditions described in the materials and methods. (B) The level of three bioactive compounds in AEAC, total phenol, flavonoid and crudal saponin were measured using the standard protocols as described in previous studies. The data shown represent the means ± SD of three replicates.

2), after which they were concentrated by vacuum evaporation and lyophilization using circulating extraction equipment (IKA Labortechnik, Staufen, Germany). Finally, the AEAC powder was dissolved in dH_2O or DMEM (Thermo Scientific, Waltham, MA, USA) to 1 mg/ml, then further diluted to the required concentration.

Analysis of bioactive compounds in AEAC

The level of three bioactive compounds in AEAC, total phenol, flavonoid and crudal saponin, were measured as described in previous studies. First, the amount of total phenol in AEAC was determined according to the Folin-Ciocalteu method [36]. Briefly, the collected sample (20 μl) was mixed with 100 μl of 0.2 N Folin-Ciocalteu reagent for 5 min, after which 300 μl of 20% sodium carbonate was added. Following incubation at room temperature for 2 hr, the absorbance of the reaction mixture was measured at 765 nm. Gallic acid was used as a standard to generate a calibration curve. Total phenolic content was expressed in milligrams of gallic acid equivalents per gram of AEAC extract.

The amount of total flavonoids in AEAC was determined according to the method described by Meda et al [28]. Briefly, AEAC (200 μl) was added to test tubes containing 60 μl of 5% potassium nitrite, 600 μl of distilled water, and 60 μl of 10% aluminum chloride. After incubation at 25°C for 5 min, the absorbance of the reaction mixture was measured at 510 nm. Total flavonoids content was determined using a standard curve with quercetin as a standard and expressed as milligrams of quercetin equivalents per gram of AEAC powder.

The total amount of crude saponin was also determined as described in previous studies [6]. Briefly, AEAC dissolved in 30 ml dH_2O was repeatedly extracted with ethyl ether (50 ml) to remove lipid soluble substances. After collection of the aqueous layer, samples were further extracted with n-butanol (30 ml) three times. This layer was concentrated by vacuum evaporation and lyophilization using circulation extraction equipment (IKA Labortechnik). Finally, the total level of crude saponin was calculated using the following equation:

Crude saponin (mg/g) = A-B/S

A: dry weight of n-butanol layer (mg), B: weight of flask (mg), S: solid volume of sample (g)

Cell culture

The BV-2 microglial cell line used in this study was macrophage cells originated from an Abelson murine leukemia virus-induced tumor obtained from the Korean Cell Line Bank (Seoul, Korea). These cells were grown in Dulbecco Modified Eagle's Medium (DMEM, Welgene, Gyeongsan-si, Korea) containing 10% fetal bovine serum (FBS, S001-01, Welgene, Gyeongsan-si, Korea), L-glutamine, penicillin, and streptomycin (Thermo Scientific, Waltham, MA, USA) in a humidified incubator at 37℃ under 5% CO_2 and 95% air.

Cell viability assay

Cell viability was determined using the tetrazolium compound 3-[4,5-dimethylthiazol-2-yl]-2,5-diphenyltetrazolium bromide (MTT) (Sigma-Aldrich Co.). To determine cell viability, BV-2 cells were seeded at a density of 5×10^4 cells/0.2 ml and grown for 24 hr in a 37℃ incubator. When the cells attained 70-80% confluence, they were treated with four different concentrations of LPS (0.1, 0.5, 1 and 5 mg/ml) for 24 hr to determine the optical concentration. Samples were either untreated (no treated group), treated with vehicle (dH_2O) or pretreated with 50 or 100 μg/ml of AEAC dissolved in dH_2O (AEAC50 and AEAC100 treated group, respectively) for 1 hr. Following incubation for 24 hr with 0.5 μg/ml of LPS, the supernatants were discarded, after which 0.2 ml of fresh DMEM media and 50 μl of MTT solution (2 mg/ml in PBS) were added to each well. The cells were then incubated at 37℃ for 4 hr. Next, formazan precipitate was dissolved in DMSO, after which the absorbance at 570 nm was read directly in the wells using a Molecular Devices VERSA max Plate reader (Sunnyvale, CA, USA). The morphological features of BV-2 cells in each treated group were also observed microscopically (Leica Microsystems, Switzerland).

Measurement of NO concentration

NO accumulation was used as an indicator of NO production in the cell culture medium using Griess reagent. Next, BV-2 cells were treated with AEAC (50 and 100 μg/ml) for 1 hr followed by LPS (0.5 μg/ml) for 24 hr. After collection of the supernatant, each sample (100 μl) was mixed with the same volume of Griess reagent (1% sulfanilamide and 0.1% *N*-(1-naphthyl)-ethylenediaminedihydrochloride in 5% phosphoric acid) and incubated at room temperature for 10 min. Finally, the absorbance at 540 nm was measured using a Molecular Devices VERSA max Plate reader (Sunnyvale, CA, USA).

Western blot analysis

Total protein of BV-2 cells was extracted using Pro-Prep Protein Extraction Solution (iNtRON Biotechnology, Seongnam, Korea), then quantified using a SMARTTM BCA Protein Assay Kit (Thermo Scientific, Waltham, MA, USA) for western blot. These proteins were separated by 4-20% sodium dodecyl sulfate-polyacrylamide gel electrophoresis (SDS-PAGE) for 2 hr, after which resolved proteins were transferred to nitrocellulose membranes for 2 hr at 40 V. Each membrane was then incubated separately at 4℃ with the following primary antibodies overnight: SAPK/JNK antibody (Cell Signaling Technology, Danvers, MA, USA), p-SAPK/JNK (Thr183/Tyr185) antibody (Cell Signaling Technology, Danvers, MA, USA), ERK (K-23) antibody (Santa Cruz Biotechnology, Inc. Santa Cruz, CA, USA), p-ERK (Thr202/Tyr204) antibody (Cell Signaling Technology, Danvers, MA, USA), p38 antibody (Cell Signaling Technology, Danvers, MA, USA), p-p38 (Thr180/Tyr182) antibody (Cell Signaling Technology, Danvers, MA, USA) and anti-actin antibody (Sigma-Aldrich Co.). Next, the membranes were washed with washing buffer (137 mM NaCl, 2.7 mM KCl, 10 mM Na_2HPO_4, and 0.05% Tween 20) and then incubated with 1:1,000 diluted horseradish peroxidase (HRP)-conjugated goat anti-rabbit IgG (Invitrogen, Carlsbad, CA, USA) at room temperature for 1 hr. Finally, membrane blots were developed using Amersham ECL Select Western Blotting detection reagent (GE Healthcare, Little Chalfont, UK). The chemiluminescence signals that originated from specific bands were detected using FluorChemi®FC2 (Alpha Innotech Co., San Leandro, CA, USA).

Enzyme-linked immunosorbent assay (ELISA) for IL-6

The concentration of IL-6 secreted from BV-2 cells was determined using an IL-6 ELISA kit (Biolegend, San Diego, CA, USA) according to the manufacturer's instructions. Briefly, BV-2 cells were treated with two different concentrations of AEAC (50 and 100 μg/ml) for 2 hr, followed by 1 μg/ml of LPS for 24 hr. After collection of the supernatant from cells, 100 ml of serial dilutions of the standard or the supernatant were added to a 96-well plate coated with anti-IL-6 antibody, then incubated for 2 hr at room temperature. After removing the unbound proteins with wash solution (Phosphate Buffered Saline (PBS), 0.05% Tween-20, pH7.4), 100 μl of avidin–horseradish peroxidase solution was added to each well, and the plates were allowed to bind at 37℃ for 2 hr. The plate was maintained at 37℃ for 30 min to react with 100 μl of substrate solution. The reaction was then stopped by the addition of 100 μl blocking solution, after which the absorbance at 450 nm was read with a microplate reader (VERSA max, Micro-reader, MDS. Co., Sunnyvale, CA, USA).

RT-PCR analysis for cytokine gene expression

The mRNA levels of inducible nitric oxide synthase (iNOS), COX-2, TNF-α, IL-1β, IL-6 and IL-10 were measured by RT-PCR as previously described. First, total RNA molecules were purified from each cultured cell using RNAzol (Tel-Test Inc., Friendswood, Texas, USA). After the quantification of the RNA using a NanoDrop system (Biospec-nano, Shimadzu Biotech, Kyoto, Japan), the expression of the target genes was assessed using RT-PCR with 5 μg of total RNA from cells of each group. Next, 500 ng of oligo-dT primer (Invitrogen, Carlsbad, CA, USA) were annealed at 70℃ for 10 min. The complementary DNA (cDNA), which was used as the template for further amplification, was synthesized by the addition of deoxyadenosine triphosphate (dATP), deoxycytidine triphosphate (dCTP), deoxyguanosine triphosphate (dGTP), and deoxythymidine triphosphate (dTTP) with 200 units of reverse transcriptase (Superscript II, 18064-014, Invitrogen, 200 U/μl). Next, 10 pmol of the sense and anti-sense primers were added, and the reaction mixture was subjected to 28-32 cycles of amplification. Amplification was conducted in a Perkin-Elmer Thermal Cycler using the following cycles: 30 sec at 94℃, 30 sec at 62℃, and 45 sec at 72℃. The primer sequences for target gene expression identification were as follows: iNOS, sense primer: 5′-CACTT GGAGT TCACC CAGT-3′, anti-sense primer: 5′-ACCAC TCGTA CTTGG GATGC-3′; COX-2, sense primer: 5′-CAGGT CATTG GTGGA GAGGT GTATC-3′, anti-sense primer: 5′-CCAGG AGGAT GGAGT TGTTG TAGAG-3′; TNF-α, sense primer: 5′-CCTGT AGCCC ACGTC GTAGC-3′, anti-sense primer: 5′-TTGAC CTCAG CGCTG ACTTG-3′; IL-1β, sense primer: 5′-GCACA TCAAC AAGAG CTTCA GGC AG-3′, anti-sense primer: 5′-GCTGC TTGTG AGGTG CTGAT GTAC-3′; IL-10, sense primer: 5′-CCAAG CCTTA TCGGA AATGA-3′, anti-sense primer: 5′-TTTTC ACAGG GGAGA AATCG-3′; IL-6, sense primer: 5′-TTGGG ACTGA TGTTG TTGACA-3′, anti-sense primer: 5′-TCATC GCTGT TGATA CAATC AGA-3′; b-actin sense primer: 5′-GTG GGG CGC CCC AGG CAC CAG GGC -3′, anti-sense primer: 5′-CTC CTT AAT GCT ACG CAC GAT TTC-3′. The experiment was repeated three times, and all samples were analyzed in

triplicate. The final PCR products were separated on 2% agarose gel and then visualized by ethidium bromide staining.

Cell cycle assay

The cell cycle was measured using a Muse™ Cell Cycle Kit (MCH100106, Millipore Co., Billerica, MA, USA) according to the manufacturer's instructions. Briefly, BV-2 cells were divided into 100 mm^2 dishes (2.5×10^6 cells/dish), then pretreated with two different concentrations of AEAC (50 and 100 μg/ml) for 1 hr. After subsequent treatment with 0.5 μg/ml LPS for 24 hr, total cells from subset groups were harvested by centrifugation at 3,000× g for 5 min, then fixed with 70% EtOH at -20℃ for 3 hr. The fixed cells were washed with PBS, then added to 200 μl of Cell Cycle Reagent. Following incubation at 37℃ in a CO_2 incubator for 30 min, cell cycles were analyzed using FACS (Millipore Co., Billerica, MA, USA).

Analysis of intracellular ROS level

Intracellular ROS levels in BV-2 cells were measured by staining with 2′,7′-dichlorofluorescein diacetate (DCFH-DA) (Sigma-Aldrich Co.), which is a cell permeable and non-fluorescent agent that can be deacetylated by intracellular esterases to nonfluorescent DCFH. In the presence of ROS, DCFH was converted to highly fluorescent DCF intracellularly. Briefly, BV-2 cells were seeded at 5×10^5 cells/2 ml in 6-well plates, then grown with two different concentrations of AEAC for 1 hr in a 37℃ incubator. After washing once with 1× PBS, the cells were incubated with 0.5 μg/ml of LPS for another 24 hr. Next, cells were incubated with 25 μM DCFH-DA for 30 min at 37℃. Finally, the cells were washed twice with PBS, after which the green fluorescence was observed at 200× and 400× magnification using a fluorescent microscope (Eclipse TX100, Nikon, Tokyo, Japan).

Statistical analysis

One-way ANOVA (SPSS for Windows, Release 10.10, Standard Version, Chicago, IL, USA) was used to identify significant differences between No and LPS treated groups, or Vehicle+LPS treated group and AEAC+LPS treated group. All values are reported as the mean ± standard deviation (SD), and a p value of <0.05 was considered significant.

Results

Bioactive compounds in AEAC

As shown in Fig. 1B, AEAC contained high concentrations of three bioactive components with anti-inflammatory activity. The concentration of total phenolic compounds and total flavonoid compounds was shown to be 1.32 mg/g and 13.8 mg/g, respectively. Furthermore, a crudal saponin was detected at 57.2 mg/g in AEAC.

Toxicity of AEAC and LSP cotreatment

Before toxicity analysis of AEAC and LPS, an optimal concentration of LPS was determined by analysis of NO concentration. The concentration of NO was consistently

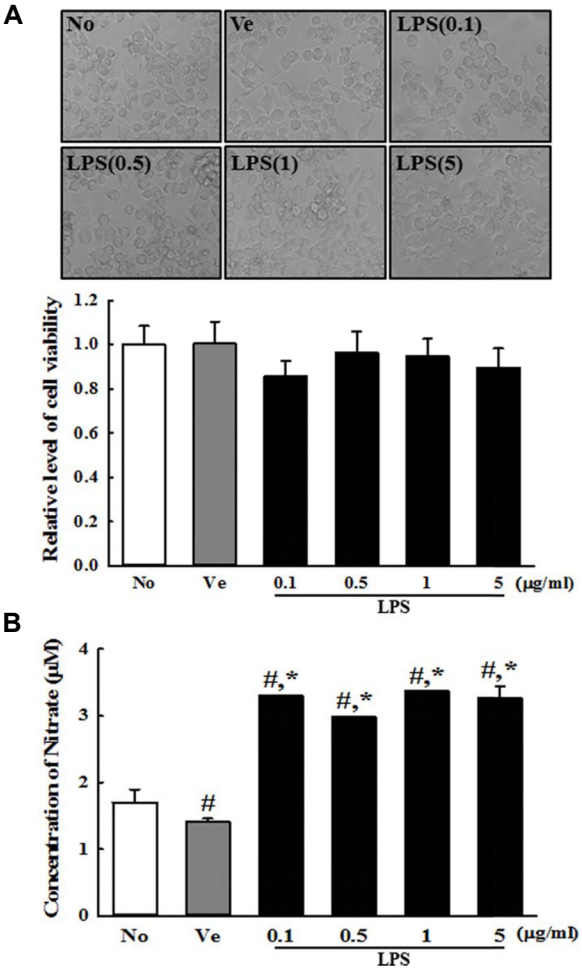

Fig. 2. Determination of the optimal concentration of LPS. (A) After incubation with different concentrations of LPS in BV-2 cells for 24 hr, their morphologies were observed under a microscope at 400× magnification. Their viability was determined by MTT assay in triplicate. (B) The level of NO was determined in supernatant collected from BV-2 cells treated with different concentrations of LPS using a NO assay kit. The data shown represent the means ± SD of three replicates. #, p<0.05 relative to the No treated group. *, p<0.05 relative to the Vehicle treated group.

found to be at high levels (131%, $p<0.05$) in all BV-2 cells treated with 0.1-5 mg/ml of LPS compared with Vehicle treated group (Fig. 2B). Moreover, LPS-treated BV-2 cells showed no significant toxicity with respect to cell morphology and viability under these conditions (Fig. 2A). Based on these results, 1 mg/ml of LPS was determined to be the optimal concentration to induce an inflammatory response.

Furthermore, the viability and morphology of BV-2 cells were consistently maintained after treatment with both concentrations of AEAC and LPS and no significant toxicity was not observed in these groups (Fig. 3). These findings indicate that AEAC showed no toxicity at less than 100 μg/ml.

Effects of AEAC on NO production, iNOS and COX-2 expression

To analyze the potential anti-neuroinflammatory properties of AEAC, alterations in NO concentration, iNOS and COX-2 expression were measured in LPS-activated BV-2 cells after AEAC pretreatment. The NO concentration was 188% higher in the Vehicle+LPS treated group than the No treated group (p=0.01). However, their level decreased by 20% (p=0.02) and 50% (p=0.01) in the AEAC pretreated group in a dose dependent manner (Fig. 4A). A similar decrease was observed in iNOS and COX-2 mRNA expression, although these patterns were not linked to dose increase (Fig. 4B). Taken together, these findings indicate that AEAC pretreatment can inhibit the increase in NO concentration, COX-2 and iNOS expression in LPS-activated BV-2 cells.

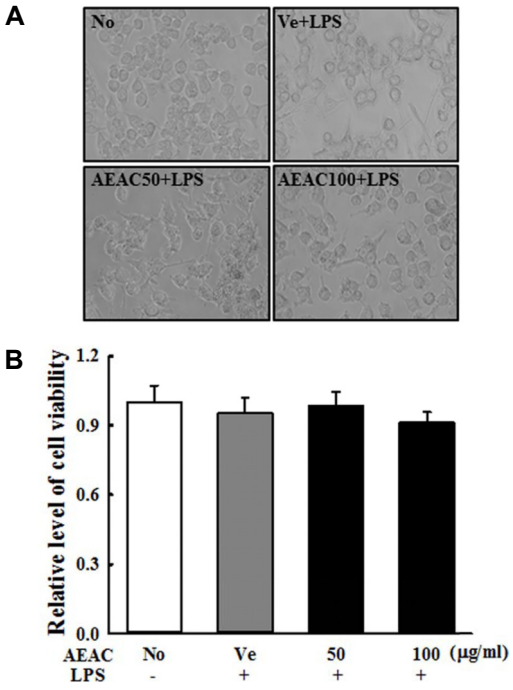

Fig. 3. Toxicity of AEAC+LPS cotreatment. After incubation with different concentrations of AEAC+LPS in BV-2 cells for 24 hr, (A) their morphologies were observed under a microscope at 400× magnification. (B) Their viability was determined by MTT assay in triplicate. The data shown represent the means ± SD of three replicates.

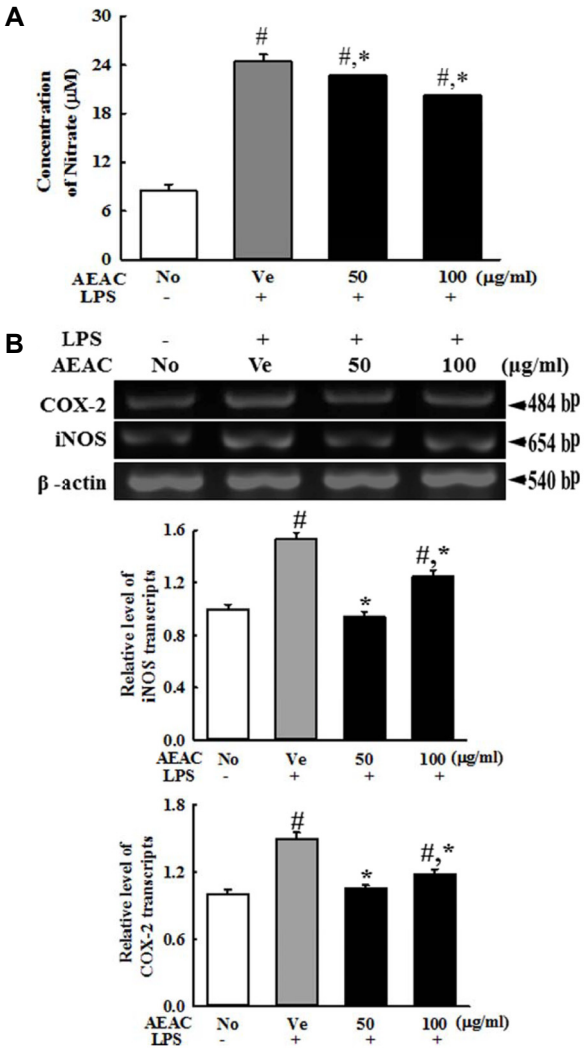

Fig. 4. Determination of NO concentration, COX-2 and iNOS expression. (A) NO concentration. The level of NO was determined in supernatant collected from LPS-stimulated BV-2 cells treated with different concentrations of AEAC using a NO assay kit. Triplicate trials per group were evaluated by NO assay. (B) RT-PCR analysis. Changes in the transcript levels of COX-2 and iNOS were examined by RT-PCR in the No, Vehicle+LPS and AEAC+LPS treated groups using specific primers. The data shown represent the means ± SD of three replicates. #, $p<0.05$ relative to the No treated group. *, $p<0.05$ relative to the Vehicle treated group.

Effects of AEAC on the expression of inflammatory cytokines

We further investigated whether AEAC can induce alterations in the expression of pro-inflammatory and anti-inflammatory cytokines. To accomplish this, the transcript levels of TNF-α, IL-1β, IL-10 and IL-6 were measured in AEAC treated BV-2 cells by RT-PCR. The expression of the four cytokines in the subset group showed a very similar pattern. The expression levels of the four transcripts were significantly higher in the Vehicle+LPS treated group than the No treated group (No treated group vs. Vehicle+LPS treated group; TNF-α: 1.00±0.05 vs. 1.16±0.02, $p<0.05$; IL-1β: 1.02± 0.03 vs. 2.46±0.24, $p<0.02$; IL-6: 1.01±0.02 vs. 3.63±0.43, $p<0.03$; IL-10: 1.02±0.03 vs. 1.36±0.14, $p<0.05$). However, these levels in most of them was decreased in the AEAC50+LPS treated group relative to the Vehicle+LPS treated group, although their decrease rate varied (Vehicle+LPS vs. AEAC50+LPS; TNF-α: 1.16±0.02 vs. 0.91±0.05, $p<0.05$; IL-1β: 2.46±0.24 vs. 1.68±0.40, $p<0.04$; IL-6: 3.63±0.43 vs. 2.97± 0.21, $p<0.05$; IL-10: 1.36±0.14 vs. 1.39±0.19, $p>0.05$, Fig. 5A). Also, a similar pattern was detected in the AEAC50+LPS treated group.

The concentration of IL-6 in the culture supernatant of BV-2 cells was further measured by ELISA to confirm the results of RT-PCR. The IL-6 concentrations reflected the results of the IL-6 transcripts in all AEAC+LPS treated groups (Vehicle+LPS treated group vs. AEAC100+LPS treated group; 400±25 vs. 253±19, $p<0.05$, Fig. 5B). These findings suggest that AEAC pretreatment suppresses the enhancement of anti- and pro-inflammatory cytokines expression induced by LPS-stimulated BV-2 cells.

Effects of AEAC on MAPK signaling pathway

The MAPK pathway plays critical roles on the inflammatory cellular responses to various cytokines in neuronal cells [25]. To investigate whether the MAP kinase pathway contributed to the anti-neuroinflammatory response of AEAC, the phosphorylation levels of ERK, JNK and p38 were measured in AEAC+LPS treated BV-2 cells by Western blotting. As shown in Fig. 6, the phosphorylation level of the three members was higher after LPS stimulation compared with No treatment, with ERK and JNK showing dramatic increases (No treated group vs. Vehicle+LPS treated group; ERK: 1.01±0.04 vs. 1.22±0.06, $p<0.03$; JNK: 1.00±0.01 vs. 1.24± 0.08, $p<0.05$; p38: 1.00±0.01 vs. 1.31±0.12, $p<0.02$). However, AEAC50 pretreatment induced recovery of the LPS-induced phosphorylation of ERK1/2, JNK and p38 protein (Vehicle+ LPS treated group vs. AEAC50+LPS treated group; ERK1/2: 1.22± 0.06 vs. 1.12±0.04, $p<0.05$; JNK: 1.24±0.08 vs. 0.88±0.06, $p<0.03$; p38: 1.31±0.03 vs. 0.97±0.05, $p<0.04$), even though the rate of decrease was greater for ERK1/2 and JNK than p38. In case of the AEAC100+LPS treated group, these recovery observed in only JNK phosphorylation. Overall, our findings

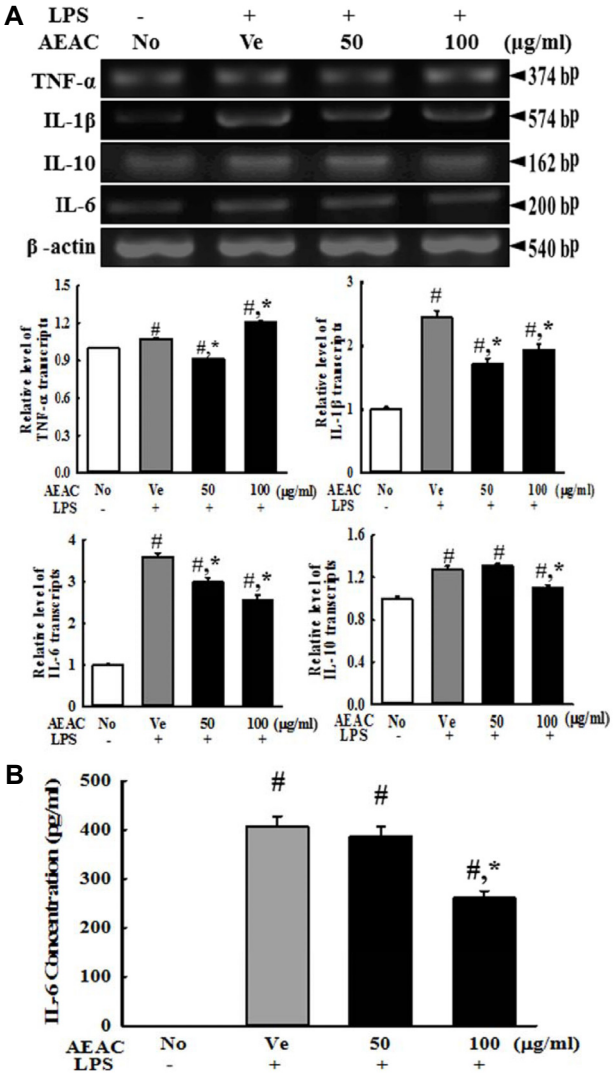

Fig. 5. Measurement of pro-inflammatory and anti-inflammatory cytokines. (A) RT-PCR analysis. The mRNA levels of the TNF-α, IL-1β, IL-10 and IL-6 genes were examined by RT-PCR in the No, Vehicle+LPS and AEAC+LPS treated group using specific primers. (B) IL-6 concentration. After collection of culture supernatant from BV-2 cells cotreated with AEAC+LPS, IL-6 concentrations were measured using an IL-6 ELISA kit that could detect IL-6 at 9.3 pg/ml. The data shown represent the means ± SD of three replicates. #, $p<0.05$ relative to the No treated group. *, $p<0.05$ relative to the Vehicle treated group.

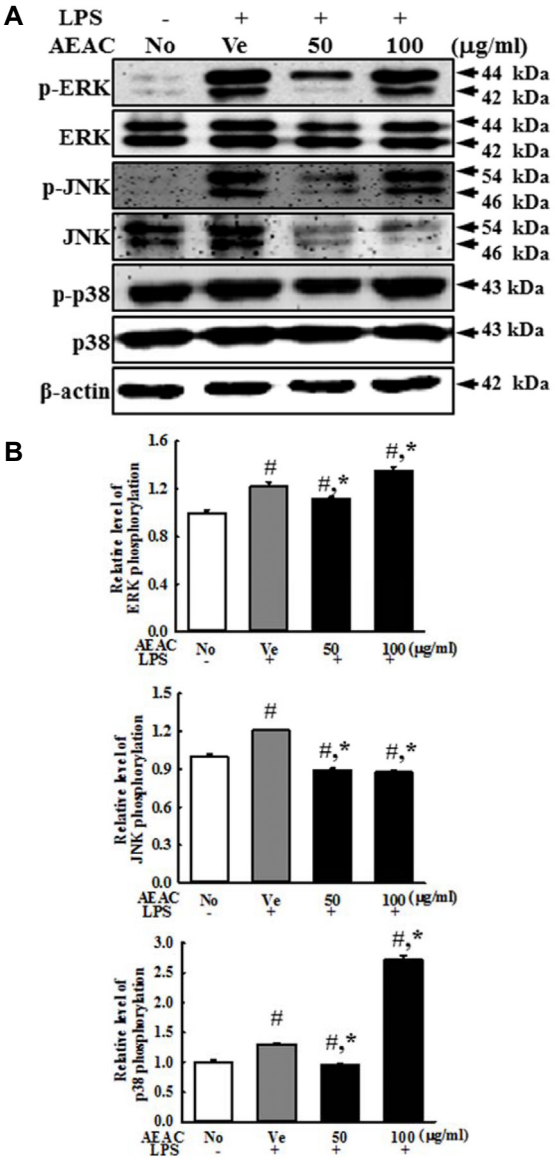

Fig. 6. Expression of three members of the MAP kinase signaling pathway. After transfer of the cell homogenates into nitrocellulose membranes, the level of p-ERK, ERK, p-JNK, JNK, p38, p-p38 and β-actin were detected with specific antibodies, followed by horseradish peroxidase-conjugated goat anti-rabbit IgG. The intensity of each band was determined using an imaging densitometer. The data represent the means ± SD of three replicates. #, $p<0.05$ relative to the No treated group. *, $p<0.05$ relative to the Vehicle treated group.

indicate that AEAC can suppress inflammatory response through the enhanced phosphorylation of MAP kinase members in LPS-stimulated BV-2 cells.

Effects of AEAC on regulation of the cell cycle

To examine whether the suppression of neuroinflammation induced by AEAC treatment can affect regulation of the cell cycle, the number of cells in each stage of the cell cycle was counted in subset groups. In the Vehicle+LPS treated group, the cell number in the G0/G1 stage was slightly decreased (No treated group vs. Vehicle+LPS treated group; 70.1±0.45 vs. 61.8±0.55, $p<0.05$), while those in the S and G2/M stage were increased (No treated group vs. Vehicle+LPS treated group; G2/M: 17.3±0.72 vs. 21.8±0.53, $p<0.05$, S: 7.1±0.33 vs. 9.1±0.47, $p<0.05$). However, AEAC+LPS cotreatment induced recovery of the number of cells in the G2/M stage (Vehicle+LPS treated group vs. AEAC100+LPS treated group; 21.8±0.53 vs. 16.5±0.45, $p<0.05$: Vehicle+LPS treated group vs. AEAC50+LPS treated group; 21.8±0.53 vs. 12.5±0.93, $p<0.05$) and G0/G1 stage (Vehicle+LPS treated group vs. AEAC100+LPS treated group; 61.8±0.55 vs. 66.5±1.12, $p<0.05$: Vehicle+LPS treated group vs. AEAC50+LPS treated group; 61.8±0.55 vs. 73.0±1.35, $p<0.05$), while that in the S stage was maintained at a constant level (Fig. 7). These results suggested that AEAC treatment can recover the arrest of the cell cycle in the G2/M stage and stimulate

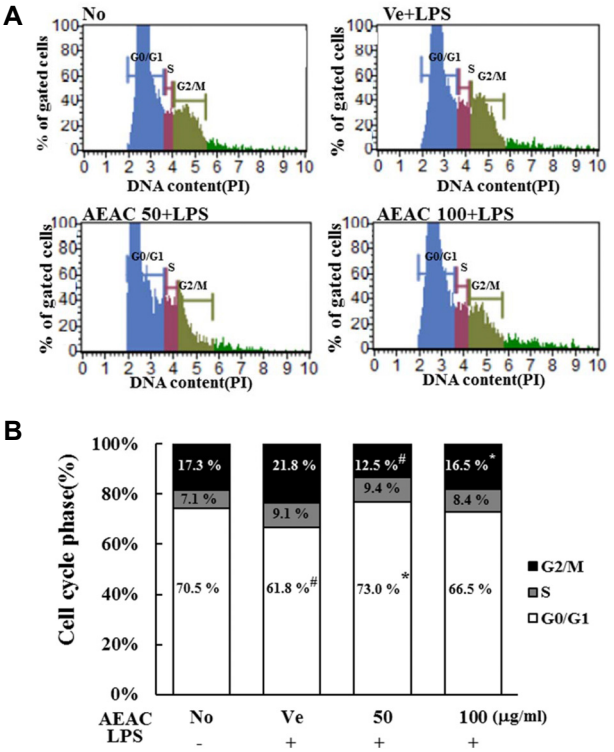

Fig. 7. Cell cycle analysis after AEAC treatment. The cell cycle distribution was determined by flow cytometric analysis of the DNA content of nuclei of BV-2 cells following staining with propidium iodide. After treatment with AEAC+LPS, the number of cells in the G0/G1, S and G2/M stage was determined.

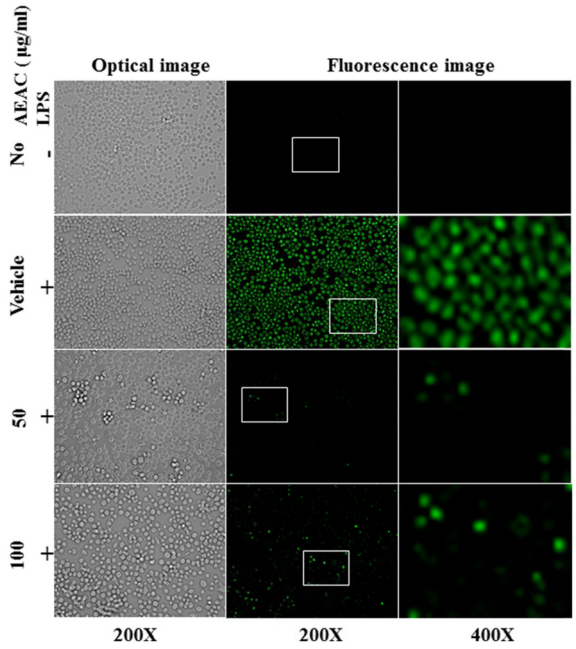

Fig. 8. Determination of intracellular ROS production. After DCFH-DA treatment, green fluorescence in cells of subset groups was observed using a fluorescent microscope (Eclipse TX100, Nikon, Tokyo, Japan). BV-2 cells in each square of a 200× magnification image (left and middle column) were further examined under 400× magnification (right column). Arrows indicate cells stained with DCFH-DA.

progression from the G2/M stage to the G1 stage.

Inhibitory effects of AEAC treatment on intracellular ROS production

Finally, we determined the inhibitory effects of AEAC against LPS-induced ROS production in BV-2 microglial cells. To accomplish this, ROS levels were measured in subset groups using a fluorescent oxidation-sensitive dye. As shown in Fig. 8, ROS production increased rapidly in the Vehicle+LPS treated group. However, this level was dramatically decreased in AEAC+LPS treated group without any significant change in their morphology. Therefore, these results indicate that increased ROS levels stimulated by LPS treatment can be effectively suppressed by AEAC pretreatment.

Discussion

The present study suggested that AEAC with high antioxidant activity can inhibit inflammatory responses of BV-2 microglia cells to LPS-induced stimulation through regulation of the MAPK signaling pathway, cell cycle and ROS production. Microglia cells treated with LPS showed enhancement of the MAPK member's phosphorylation, arrest of cell cycle and increase of ROS production, which subsequently led to the up-regulation of NO, iNOS, COX and inflammatory cytokines. However, AEAC cotreatment significantly inhibited the inflammatory responses to LPS in BV-2 microglia cells through recovery of the MAPK signaling pathway, cell cycle and intracellular ROS production. Thus, our results indicated that AEAC is important for the neuroinflammatory responses, suppression and cell cycle recovery in response to LPS and may be therapeutic drugs for neurodegenerative diseases.

The root of *A. cochinchinesis* retains 19 amino acids, polysaccharides, and more than 20 multi-functional compounds. Among these, functional compounds include β-sitosterol [21], daucosterol [30], n-ethatriacontanoic acid [37], palmitic acid [20], 9-heptacosylene [44], smilagenin [1], diosgenin [3], sarsasapogenin-3-O-β-D-glucoside feeding grapes imidacloprid [43], 5-methoxy methyl furfural, yame sapogenin, diosgenin-3-O-β-D imidacloprid feeding glucose glycosides [34, 42], aspacochioside D [35], iso-agatharesinoside [19] and seven steroidal saponins [47]. In addition, the polysaccharide composites of *A. cochinchinesis* roots have several therapeutic properties including (1) antioxidant and anti-aging [30-32], (2) antibacterial-inflammatory effects [18], (3) antitumor effects [14, 22, 39], (4) blood sugar reducing activity [46] and (5) improvement of cough [23, 24]. Furthermore, three novel pregnane glycosides including aspacochinosides N, O and P and four known furostanol glycosides were isolated from the roots of *A. cochinchinesis* [9]. Although the distribution of many compounds in the roots of *A. cochinchinesis* have been consistently reported, few studies have investigated its effects on anti-neuroinflammation. Only one study showed the production of NO in LPS-induced BV-2 cells was significantly inhibited by treatment with compounds 2, 3 and 4 [9]. In our studies, the concentration of total flavonoids, total phenols and crudal saponins in the extract of *A. cochinchinesis* roots were measured to determine if there was a correlation between anti-oxidant activity and anti-neuroinflammation effect. The anti-neuroinflammatory effects of AEAC have been investigated based on an inflammatory mediators including NO, TNF-α, IL-1β, iNOS, and COX-2, as has its ability to influence the MAPK signaling pathway, cell cycle and ROS production.

Microglia cells are major response immune cells with dual

effects in the CNS. Under normal conditions, these cells contribute to immune surveillance and host defense against infected pathogens [31]. However, under pathological conditions, activated microglia cells are involved in neurological damage via the production of various pro-inflammatory factors and cytotoxic regulators including NO, TNF-α, COX-2, IL-1β and ROS [10, 29]. Furthermore, there have been some controversial findings regarding the role of microglia cells under these conditions because inflammation has dual effect in many diseases. Some studies have shown that microglia triggered by damaged or dead neurons induced a reduction of neuronal injury and stimulation of tissue repair [25, 29], while others have suggested the neurotoxic effects of activated microglia cells after neuronal damage [12, 33, 45]. Therefore, suppression of the inflammatory process in microglia cells may be a key therapeutic target to alleviate the progression of the neurological diseases. In our study, we selected LPS-activated BV-2 mouse neuroglia cells that mimic inflammation as a cellular model for investigation of potential therapeutic drugs for neuroinflammatory diseases. Treatment of these cells with LPS successfully induced neuroinflammatory responses, including increased NO concentration, TNF-α expression, IL-1β expression and COX-2 expression as in previous studies.

The beneficial effects of several herbal medicines on neuroprotection have been reported as part of the development of novel therapeutic drugs for neurodegenerative diseases. An extract of *Tripterygium wilfordii* Hook markedly attenuated the production of TNF-α, IL-1β, NO, prostaglandin E2 (PGE2) and intracellular SOD and inhibited the expression of iNOS and COX-2 [5]. Additionally, Gua Lou Gui Zhi decoction inhibited LPS-induced inflammatory response in microglial cells through the reduction of NO, TNF-α, IL-6 and IL-1β production [38]. Some similar effects on the inhibition of LPS-induced production of pro-inflammatory mediators were detected in microglia cells treated with active compounds of *Erigeron breviscapus* (Vant.) Hand-Mazz [32], *Ligusticum chuanxiong* [17] and ginseng [8]. In the present study, AEAC treatment induced similar neuroprotective effects on changes in inflammatory mediators including NO, TNF-α, IL-1β and iNOS in the LPS-stimulated BV-2 microglia cells. The results of our study also showed that AEAC can recover alterations in the MAPK signaling pathway, cell cycles and production of ROS in the same cells. However, more studies are required to identify single compounds with anti-neuroinflammation activity as well as evaluate the therapeutic effects in animal models with neurodegenerative diseases.

In summary, the present study investigated the effects of neuroprotection by AEAC, particularly its anti-neuroinflammatory mechanism in BV-2 microglia cells. AEAC inhibited the production of pro-inflammatory mediators such as NO, COX-2 and cytokines through regulation of the MAPK signaling pathway and inhibition of ROS production. This is also the first study to report that the inhibitory effects of AEAC associated with recovery of cell cycle arrest.

Acknowledgement

This work was supported by a 2-Year Research Grants of Pusan National University.

The Conflict of Interest Statement

The authors declare that they have no conflicts of interest with the contents of this article.

References

1. Cong, P. Z. and Keman, S. 2000. Handbook of Analytical Chemistry - Mass, pp. 296-298, 2nd ed., Chemical Industry Publishing House, Beijing, China.
2. Frank-Cannon, T. C., Alto, L. T., McAlpine, F. E. and Tansey, M. G. 2009. Does neuroinflammation fan the flame in neurodegenerative diseases? *Mol. Neurodegener.* **4**, 47-60.
3. Gong, Y. H. 1986. 13C NMR Chemical Shifts of Natural Organic Compounds. pp. 252, 2nd ed., Yunnan Science and Technology Publishing House, Kunming, China.
4. Graeber, M. B., Li, W. and Rodriguez, M. L. 2011. Role of microglia in CNS inflammation. *FEBS Lett.* **585**, 3798-3805.
5. Haixia, H., Zuanfang, L., Xiaoqin, Z., Ruhui, L., Jiumao, L., Jun, P., Jing, T. and Lidian, C. 2013. Gua Lou Gui Zhi decoction suppresses LPS-induced activation of the TLR4/NF-kB pathway in BV-2 murine microglial cells. *Int. J. Mol. Med.* **31**, 1327-1332.
6. Hassan, S. M., Al Aqil, A. A. and Attimarad, M. 2013. Determination of crude saponin and total flavonoids content in guar meal. *Adv. Med. Plant Res.* **1**, 24-28.
7. Hong, H., Kim, B. S. and Im, H. I. 2016. Pathophysiological role of neuroinflammation in neurodegenerative diseases and psychiatric disorders. *Int. Neurourol. J.* **20**, S2-7.
8. Hyun, M. S., Hur, J. M., Shin, Y. S., Song, B. J., Mun, Y. J. and Woo, W. H. 2009. Comparison study of white ginseng, red ginseng, and fermented red ginseng on the protective effect of LPS-induced inflammation in RAW 264.7 cells. *J. Appl. Biol. Chem.* **52**, 21-27.
9. Jian, R., Zeng, K. W., Li, J., Li, N., Jiang, Y. and Tu, P. 2013.

Anti-neuroinflammatory constituents from *Asparagus cochinchinensis*. *Fitoterapia* **84**, 80-84.
10 .Jin, R., Yang, G. and Li, G. 2010. Inflammatory mechanisms in ischemic stroke: role of inflammatory cells. *J. Leukoc. Biol.* **87**, 779-789.
11. Jung, K. H., Choi, H. L., Park, S. J., Lee, G. H., Kim, M. R., Min, J. K., Min, B. I. and Bae, H. S. 2014. The effects of the standardized herbal formula PM014 on pulmonary inflammation and airway responsiveness in a murine model of cockroach allergen-induced asthma. *J. Ethnopharmacol.* **155**, 113-122.
12. Kaushal, V. and Schlichter, L. C. 2008. Mechanisms of microglia-mediated neurotoxicity in a new model of the stroke penumbra. *J. Neurosci.* **28**, 2221-2230.
13. Kim, H. M., Lee, E. H., Lim, T. K., Jung, J. A. and Lyu, Y. S. 1998. Inhibitory effect of *Asparagus cochinchinensis* on tumor necrosis factor-alpha secretion from astrocytes. *Int. J. Immunopharmacol.* **20**, 153-162.
14. Koo, H. N., Jeong, H. J. and Choi, J. Y. 2000. Inhibition of tumor necrosis factor-a-induced apoptosis by *Asparagus cochlnchinensis* in Hep G2 cells. *J. Ethnopharmacol.* **73**, 137-143.
15. Lee, D. Y., Choo, B. K., Yoon, T. S., Cheon, M. S., Lee, H. W., Lee, Y. A. and Kim, H. K. 2009. Anti-inflammatory effects of *Asparagus cochinchinensis* extract in acute and chronic cutaneous inflammation. *J. Ethnopharmacol.* **121**, 28-34.
16. Lee, H. A., Kim, J. E., Song, S. H., Sung, J. E., Kim, D. S., Son, H. J., Lee, C. Y., Lee, H. S. and Hwang, D. Y. 2016. Effects of aqueous extract from *Asparagus cochinchinensis* on regulation of nerve growth factor in neuronal cells. *J. Life. Sci.* **26**, 509-518.
17. Lee, K. W., Jung, S. Y., Choi, S. M. and Yang, E. J. 2012. Effects of ginsenoside re on LPS induced inflammatory mediators in BV2 microglial cells. BMC Complement. *Altern. Med.* **12**, 196.
18. Li, M., Fei, Y. and Wang, J. K. 2005. Studies on pharmacologic effects of *Radix Asparagi. LiShiZhen Med. Mater. Med. Res.* **16**, 580-582.
19. Li, X. N., Chu, C., Cheng, D. P., Tong, S. Q. and Yan, J. Z. 2012. Norlignans from *Asparagus Cochinchinensis*. *Nat. Prod. Commun.* **7**, 1357-1358.
20. Liang, Z. Z., Aquino, R., De Simone, F., Dini, A., Schettino, O. and Pizza, C. 1988. Oligo furo stanosides from *Asparagus cochinchinensis*. *Planta Med.* **54**, 344-346.
21. Liu, Y. Z., Qu, F. Y. and Zhang, P. X. 2001. Effect of chloroform extract of Tiandong on the brain antioxidation of D-galatose-induced senile mice. *Heilongjiang Med. Pharm.* **24**, 7-8.
22. Luo, J., Long, Q. D., Li, C. X., Li, L. and Huang, N. H. 2000. Inhibitory effects of ALWB and ACM on mice bearing tumor. *J. GuiYang Med. Coll.* **25**, 15-16.
23. Luo, J., Long, Q. D., Li, C. X., Li, L., Huang, N. H., Nie, M. and Tang, P. X. 1998. Comparison of antitussive, expectorant and anti-asthmatic effect between ALWB and ACM. *J. GuiYang Med. Coll.* **23**, 132-134.
24. Lv, B. and Liu, W. Z. 2004. Aspartate treatment of hemodialysis patients with hypertension in 22 cases. *J. Tradit. Chin. Med.* **19**, 43-44.
25. Majumdar, A., Cruz, D., Asamoah, N., Buxbaum, A., Sohar, I., Lobel, P. and Maxfield, F. R. 2007. Activation of microglia acidifies lysosomes and leads to degradation of Alzheimer amyloid fibrils. *Mol. Biol. Cell* **18**, 1490-1496.
26. McGeer, P. L., Kawamata, T., Walker, D. G., Akiyama, H., Tooyama, I. and McGeer, E. G. 1993. Microglia in degenerative neurological disease. *Glia* **7**, 84-92.
27. McGeer, P. L. and McGeer, E. G. 1995. The inflammatory response system of brain: implications for therapy of alzheimer and other neurodegenerative diseases. *Brain Res. Brain Res. Rev.* **21**, 195-218.
28. Meda, A., Lamien, C. E., Romito, M., Millogo, J. and Nacoulma, O. G. 2005. Determination of the total phenolic, flavonoid and proline contents in Burkina Fasan honey, as well as their radical scavenging activity. *Food Chem.* **91,** 571-577.
29. Neumann, J., Sauerzweig, S., Rönicke, R., Gunzer, F., Dinkel, K., Ullrich, O., Gunzer, M. and Reymann, K. G. 2008. Microglia cells protect neurons by direct engulfment of invading neutrophil granulocytes: a new mechanism of CNS immune privilege. *J. Neurosci.* **28**, 5965-5975.
30. Ni, J. M., Zhao, R. and Wang, R. 1992. Comparison on amino acid content in prepared and unprepared *Asparagus cochinchinensis*. *Chin. Tradit. Herb Drugs* **23**, 182-183.
31. Olson, J. K. and Miller, S. D. 2004. Microglia initiate central nervous system innate and adaptive immune responses through multiple TLRs. *J. Immunol.* **173**, 3916-3924.
32. Or, T. C., Yang, C. L., Law, A. H., Li, J. C. and Lau, A. S. 2011. Isolation and identification of anti-inflammatory constituents from ligusticum chuanxiong and their underlying mechanisms of action on microglia. *Neuropharmacology* **60**, 823-831.
33. Qu, F. Y., Wei, X. D., Li, S. L., Wang, Y. M. and Bai, S. G. 1999. Experimental study of *Asparagus cochinchinensis* delay aging. *Acta. Chin. Med. Pharm.* **2**, 68-70.
34. Shen, Y., Chen, H. S. and Wang, Q. 2007. Studies on chemical constituents of *Asparagus cochinchinensis*(II). *J. Second Med. Univ.* **28**, 1241-1244.
35. Shen, Y., Xu, C. l., Xuan, W. D., Li, H. L., Liu, R. H., Xu, X. K. and Chen, H. S. 2011. A new furostanol saponin from *Asparagus cochinchinensis*. *Arch. Pharm. Res.* **34**, 1587-1591.
36. Singleton, V. L., Orthofer, R. and Lamuela-Raventos, R. M. 1999. Analysis of total phenols and other oxidation substrates and antioxidants by means of Folin-Ciocalteu reagent. *Methods Enzymol.* **299**, 152-178.
37. Tenji, K. and Junzo, S. 1979. Studies on the constituents of *Asparagi Radix. I.* On the structures of furostanol oligosides of *Asparagus cochinchinensis* (Lour.) Merr. *Chem. Pharm. Bull.* **27**, 3086-3094.
38. Wang, S., Wang, H., Guo, H., Kang, L., Gao, X. and Hu, L. 2011. Neuroprotection of scutellarin is mediated by inhibition of microglial inflammatory activation. *Bioscience* **185**, 150-160.
39. Wen, J. Y., Li, Y., Ding, S. S. and Li, Q. H. 1993. Nine pharmacological screening of medicinal plants of China *Liliaceae*

Asparagus. J. Acta. Acad. Med. Shanghai. **20**, 107-111.
40. Xiao, P. G. 2002. Modern Chinese Material Medica. pp. 150, 2nd ed., Chemical Industry Press, Beijing, China.
41. Xiong, D. S., Yu, L. X., Yan, X., Guo, C. and Xiong, Y. 2011. Effects of root and stem extracts of *Asparagus cochinchinensis* on biochemical indicators related to aging in the brain and liver of mice. *Am. J. Chinese Med.* **39**, 719-726.
42. Xu, C. L., Chen, H. S. and Tan, X. Q. 2005. Studies on the active constituents of *Asparagi Radix*. *Nat. Prod. Res. Dev.* **17**, 128-130.
43. Yang, M. H. 1981. Steroidal sapogenins of dioscorea. *Chin. Tradit. Herb Drugs* **12**, 43-44.
44. Yang, Y. C., Huang, S. Y. and Shi, J. G. 2002. Two new furostanol glycosides from *Asparagus cochinchinensis*. *Chin. Chem. Lett.* **12**, 1185-1188.
45. Yenari, M. A., Xu, L., Tang, X. N., Qiao, Y. and Giffard, R. G. 2006. Microglia potentiate damage to blood-brain barrier constituents improvement by minocycline *in vivo* and *in vitro*. *Stroke* **37**, 1087-1093.
46. Yu, F. R., Lian, X. Z. and Guo, H. Y. 2006. Effect of lucid asparagus extract on the regulation of blood sugar. *Chin. J. Clin. Rehabil.* **10**, 57-59.
47. Zhu, G. L., Hao, Q., Li, R. T. and Li, H. Z. 2014. Steroidal saponins from the roots of *Asparagus cochinchinensis*. *Chin. J. Nat. Med.* **12**, 213-217.

초록 : Lipopolysaccharide로 자극된 BV-2 미세교세포에서 신경염증 매개체, MAP kinase경로, 세포주기의 조절에 의한 천문동(*Asparagus cochinchinensis*)의 저해효과

이현아[1] · 김지은[1] · 최준영[1] · 성지은[1] · 윤우빈[1] · 손홍주[2,4] · 이희섭[3,4] · 강현구[5] · 황대연[1,4]*
([1]부산대학교 바이오소재과학과, [2]부산대학교 생명환경화학과, [3]부산대학교 식품영양학과, [4]부산대학교 웰빙제품 연구센터, [5]충북대학교 수의과대학)

미세교세포(Microglial cells)에서 신경염증반응(neuroinflammatory responses)의 억제는 알츠하이머질환, 파킨슨질환, 헌팅턴질환과 같은 신경퇴행성질환(neurodegenerative diseases)을 치료하기 위한 주요 표적으로 고려되고 있다. 천문동(*Asparagus cochinchinesis*)은 열, 기침, 신장 질환, 유방암, 염증성질환 및 뇌질환을 치료하는 데 오랫동안 사용 되어온 전통 치료제(Traditional medicine)이다. 본 연구에서는 lipopolysaccharide (LPS)로 활성화된 BV-2 미세교세포에서 항염증효과가 있는 천문동 뿌리 열수추출물(Aqueous extract from *A. cochinchinesis* root, AEAC)의 신경보호 메커니즘을 연구하였다. 먼저, 어떤 유의적인 세포독성은 플라보노이드(flavonoid), 페놀(phenol), 사포닌(saponin)을 함유하는 AEAC를 4가지 농도로 처리된 BV-2세포에서 검출되지 않았다. 또한, nitric oxide (NO), cyclooxygenase-2 (COX-2) mRNA 및 inducible nitric oxide synthase (iNOS) mRNA 수준은 AEAC+LPS 처리군에서 비하여 21%정도 감소하였다. 전염증성 사이토카인(TNF-α과 IL-1β) 및 항염증성 사이토카인(IL-6와 IL-10)농도에 대한 유사한 감소는 비록 감소비율은 다르지만, Vehicle+LPS 처리군에 비해 AEAC+LPS 처리군에서 검출되었다. 더불어, LPS 처리 후 mitogen-activated protein (MAP) kinase의 인산화수준의 증가는 AEAC 전처리군에서 유의하게 회복되었고, 세포주기에서 G2/M의 억제(arrest)는 AEAC+LPS 처리군에서 개선되었다. 또한, LPS 처리로 유도된 ROS의 증가도 AEAC 전처리군에서 감소되었다. 따라서, 이러한 결과는 AEAC가 MAPK 신호전달 경로, 세포주기 및 ROS (reactive oxygen species) 생성의 조절을 통해 LPS 자극에 대한 항신경염증 활성을 유도함을 제시하고 있다.